

Effect of Light Elements to Heterogeneity of Attenuation in the Earth's Inner Core

*Chao Liu¹, Takashi Yoshino¹

1. Institute For Planetary Materials, Okayama University

Seismic observations have provided strong evidence of hemisphere variations, showing less attenuation, and lower seismic P-wave velocity in the western hemisphere than in the eastern hemisphere in the uppermost 100 km of the inner core (Deuss, 2014; Poupinet, Pillet, & Souriau, 1983; Souriau, 2015; Tanaka & Hamaguchi, 1997). Two major hypotheses have been proposed to explain these features: (a) inner core translation, wherein eastern hemisphere is melting at the surface of the inner core and the other side is solidifying (Monnereau, Calvet, Margerin, & Souriau, 2010), partial melting may play a key role to produce such attenuation heterogeneity at the inner core boundary; (b) thermochemical convection occurs (Alboussière et al., 2010; Deuss, 2014), which may cause the distribution of light elements. Therefore, knowledge of alloy with partial molten texture and anelastic behavior of light elements-bearing alloy is necessary to constrain the heterogeneity in the Earth's inner core. As sulfur and silicon have been considered to be more probable candidates of light elements in the inner core (Miller, 2009; Poirier, 1994; Sakamaki et al., 2016; Tsuchiya & Fujibuchi, 2009), we investigated the attenuation behavior of iron alloy containing these elements.

Three different alloys (iron, S-bearing, Si-bearing alloy) were studied. Starting materials, for S- and Si-bearing alloys were synthesized at 1 GPa in a piston cylinder apparatus. The S-bearing alloy was used to investigate anelastic behavior of the partial molten state. The measurement of seismic attenuation was conducted by in situ X-ray radiographic observation at 1.6 GPa and up to 1473 K using the deformation-DIA press at the bending magnet beam line BL04B1 at SPring-8 (Yoshino et al., 2016). The alumina aggregate, sapphire single crystal and forsterite single crystal were used as a reference material in a series of experiments. The periods of oscillation were from 0.5 to 100 s.

Pure iron with average grain size, 10 μm , showed no frequency dependence of seismic attenuation factor Q^{-1} in bcc phase, and weak temperature dependence. For S-bearing samples with initially partial molten texture, melt separation occurred during experiment. The attenuation information of partial molten state could not be obtained. Attenuation of Si-bearing samples (average grain size larger than 1 mm) became larger with increasing Si-concentration, and showed no frequency and temperature dependences.

The experimental results showed that the seismic attenuation of Fe alloy is not frequency (0.01-2 Hz) dependent, which is consistent with the observed seismic data that there is no frequency dependence in some range of frequency due to different relaxation time in the uppermost inner core (Li & Cormier, 2002; Souriau & Roudil, 1995). The silicon can influence the heterogeneity of attenuation in the Earth's inner core. If silicon is one of the dominant light elements in the core, which means the concentration of silicon in west hemisphere is higher than it in east hemisphere in the uppermost 100 km of the inner core combined with the sound velocity data of Si-bearing alloy (Lin, 2003). So it can support the opinion that the core freezes in western hemisphere in uppermost of the inner core, growing the solid inner core and releasing silicon (Gubbins et al., 2011; Monnereau et al., 2010). It is needed to constrain the relationship between seismic attenuation and molten state.

Keywords: heterogeneity, inner core, attenuation, light element, partial melting

Effect of dislocation on rock anelasticity: Analogue experiment using organic polycrystals

*Yuto Sasaki¹, Yasuko Takei¹, Christine McCarthy², Ayako Suzuki¹

1. Earthquake Research Institute, University of Tokyo, 2. Lamont-Doherty Earth Observatory, Columbia University

Seismic wave velocity and attenuation are affected by the elastic and anelastic properties of rocks. Therefore, detailed mechanism of elasticity and anelasticity has to be clarified in order to estimate the state of the Earth's interior from seismic observations. Two major mechanisms of rock anelasticity have been proposed: grain boundary sliding and dislocation motion. Grain boundary and dislocation (plane and line defects, respectively) in a rock slide and dissipate the energy, causing dispersion and attenuation of the seismic wave. Due to the lack of experimental data of anelasticity of rock with dislocations (only [1] and [2]), it is difficult to elucidate the mechanism of dislocation damping. In this study, dislocation-induced anelasticity was measured accurately over a broad frequency range by using a rock analogue.

In this study, polycrystalline borneol [3] was used as a rock analogue. Effect of grain boundary sliding on the anelasticity of this material have been clarified well [4, 5, 6], making it possible to investigate the effect of dislocation by the difference from the grain boundary effect. Following three experiments were performed.

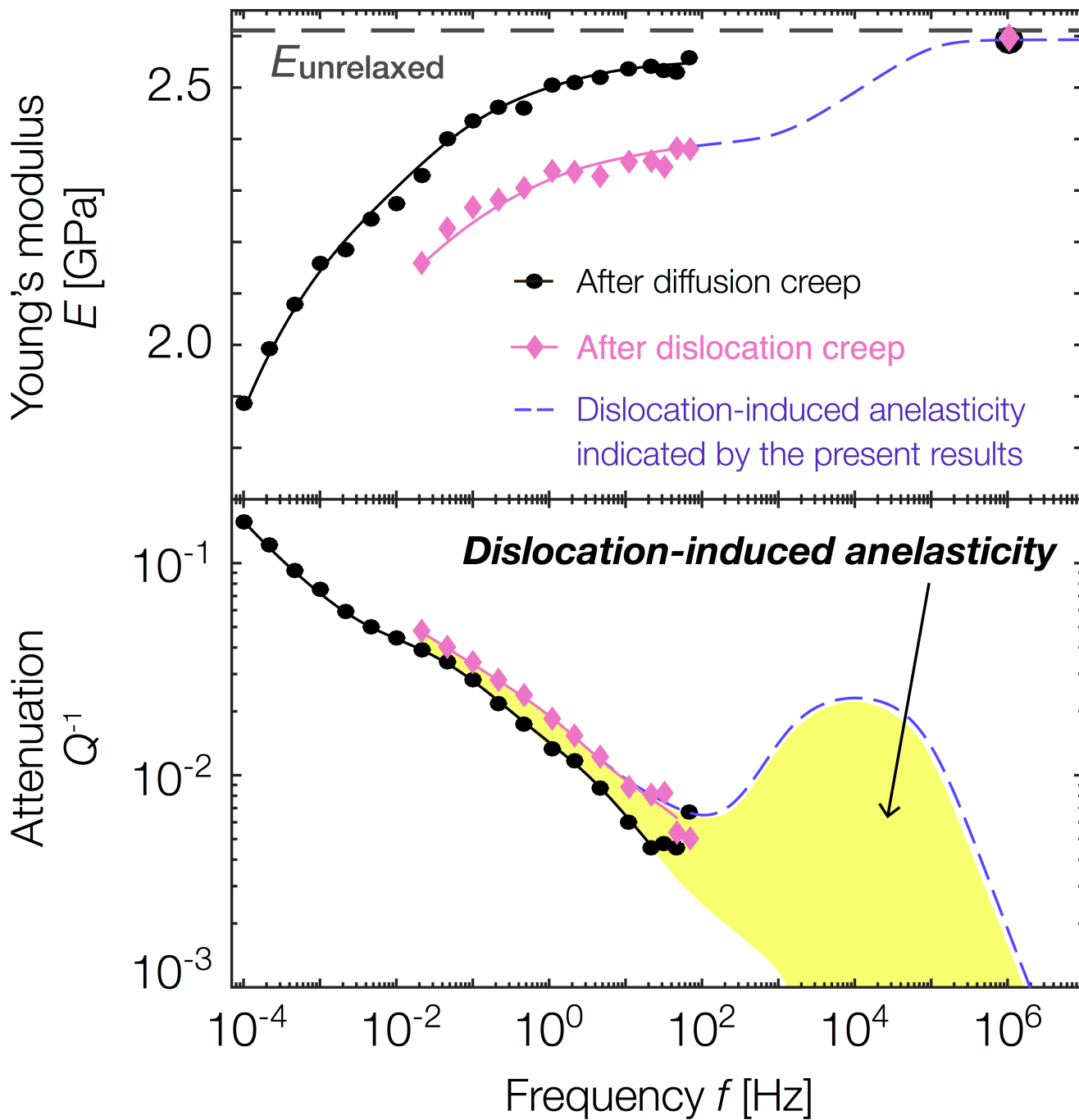
First, a deformation mechanism map of borneol was investigated in order to clarify the temperature and stress condition for the dislocation creep. Flow law (relationship between deviatoric stress σ and strain rate $d\varepsilon/dt$) of borneol was determined at 40°C and 50°C by uniaxial compression tests under a confining pressure of 0.8 MPa. As a result, a transition from diffusion creep to dislocation creep ($d\varepsilon/dt \propto \sigma^5$) was observed at about $\sigma = 1$ MPa at 50°C. Microstructure of the sample deformed under the power law regime also implied an occurrence of dislocation-induced grain boundary migration.

Second, by using a sample deformed in the dislocation creep regime, effect of dislocations on anelasticity was investigated at 10^{-4} – 10^2 Hz. Three creep tests with $\sigma = 0.27$ MPa (diffusion creep regime), $\sigma = 1.3$ MPa (transitional regime) and $\sigma = 1.9$ MPa (dislocation creep regime) were conducted on the same sample in the increasing order, and anelasticity of this sample after each creep test was measured by using a forced oscillation apparatus [5]. Young's modulus E and attenuation Q^{-1} (anelasticity) were measured at frequencies ranging from 10^{-4} to 10^2 Hz. The result shows that as σ increased, E decreased and Q^{-1} increased. These changes, however, almost fully recovered within two weeks. Therefore, it is considered that anelasticity was enhanced due to the dislocations introduced during the dislocation creep and was recovered due to dislocation recovery (annihilation) during the forced oscillation tests.

Third, in order to constrain the frequency range of the dislocation-induced anelastic relaxations, Young's modulus E at 10^6 Hz was measured before and after the dislocation creep ($\sigma = 1.9$ MPa), by the ultrasonic method. The obtained Young's modulus at 10^6 Hz was not changed by dislocations, showing that dislocation-induced anelasticity is localized to 10^2 – 10^6 Hz. This frequency range is higher than grain-boundary-induced anelasticity. Total relaxation strength of dislocation-induced anelasticity obtained in this study was $\approx 0.1E$.

- [1] Guéguen *et al.* (1989), Q^{-1} of forsterite single crystals, *Phys. Earth Planet. Inter.*
- [2] Farla *et al.* (2012), Dislocation damping and anisotropic seismic wave attenuation in Earth's upper mantle, *Science*.
- [3] Takei (2000), Acoustic properties of partially molten media studied on a simple binary system with a controllable dihedral angle, *J. Geophys. Res.*
- [4] McCarthy *et al.* (2011), Experimental study of attenuation and dispersion over a broad frequency range: 2. The universal scaling of polycrystalline materials, *J. Geophys. Res. Solid Earth*.
- [5] Takei *et al.* (2014), Temperature, grain size, and chemical controls on polycrystal anelasticity over a broad frequency range extending into the seismic range, *J. Geophys. Res. Solid Earth*.
- [6] Yamauchi and Takei (2016), Polycrystal anelasticity at near-solidus temperatures, *J. Geophys. Res. Solid Earth*.

Keywords: anelasticity, dislocation, seismic attenuation, analog experiment, defect, polycrystal



Intrinsic Attenuations in the Oceanic Lithosphere and Asthenosphere Constrained by Seismogram Envelopes

*Nozomu Takeuchi¹, NOMan Project Team

1. Earthquake Research Institute, University of Tokyo

It is widely accepted that the oceanic lithosphere and asthenosphere have high-Q and low-Q, respectively, however, it is not very clear to which extent such attenuations are affected by seismic wave scattering (e.g., Shito et al. 2015, JGR; Kennett and Furumura 2013, GJI). To distinguish the intrinsic and scattering attenuations, analyzing seismogram envelopes is known to be effective. We deployed broadband ocean bottom seismometers on the old Pacific seafloor between 2010-2014 (NOMan Project, <http://www.eri.u-tokyo.ac.jp/yesman/>). We had quite large number of aftershocks of 2011 Great Tohoku Earthquake and succeeded in obtaining envelopes of Po/So and T-phase at various distances. The data purely sample the old ocean, which should provide unique opportunities to quantitatively constrain the attenuations in the ocean. We applied our envelope simulation method (Takeuchi 2016, JGR) and obtained the attenuation model by grid-searching the best structural parameters to explain the observations.

One of the most unique features of Po/So is that spatial attenuation (i.e., energy loss rate per unit propagating distance) is independent from wave type (P- or S-wave) and frequency (Butler 1987, JGR). Several previous studies (e.g. Sereno & Orcutt 1987, JGR; Mallick & Frazer 1990, GJI) explained such features by slightly ad-hoc attenuation models (strong frequency dependency; larger P attenuations than S). In contrast, we tried to explain the observations without such assumptions and succeeded in explaining most of the observed features. The results suggest that the saturation of backscattering coefficients at higher wavenumbers is primarily responsible for the constant spatial attenuation.

Keywords: attenuation, scattered wave

Seismic attenuation structure beneath Nazca Plate subduction zone in S. Peru

*Hyoihn Jang¹, Younghee Kim¹, Robert Clayton²

1. School of Earth and Environmental Sciences, Seoul National University, 2. Division of Geological and Planetary Sciences, California Institute of Technology

We estimate seismic attenuation in terms of quality factors, QP and QS using P and S phases, respectively, recorded from Peru Subduction Experiment (PeruSE) array deployed above Nazca Plate subduction zone between 13°S and 18°S latitude in S. Peru. We first relocate 285 earthquakes with magnitude ranges of 4.0–6.0 and depth ranges of 20–250 km. We then assume a double-corner frequency source model to measure t^* , which is an integrated attenuation through the seismic raypath between the regional earthquakes and stations. The measured t^* are inverted to construct three-dimensional attenuation structures of S. Peru. Checkerboard test results for both QP and QS structures show that we have good resolution in the slab-dip transition zone between flat and normal slab subduction down to a depth of 120 km. Both QP and QS results show high attenuation in the mantle wedge along the normal slab-dip region. Also, both show relatively higher attenuation continued down to a depth of 100 km beneath volcanic arc and also beneath the Quimsachata volcano, located farther away from the arc. We plan to compare our results with velocity models previously derived from various tomography studies for understanding structural heterogeneity, thermal conditions, and fluid content in the study area. Also, we relate measured attenuation in the mantle wedge to material properties such as viscosity to understand the subduction zone dynamics.

Keywords: attenuation, Peru

Detailed seismic attenuation structure beneath Kii peninsula, southwestern Japan

*Saeko Kita¹, Takuo Shibutani²

1. Department of Earth and Planetary Systems Science, Hiroshima University, 2. Disaster Prevention Research Institute, Kyoto University

Three-dimensional seismic attenuation structure (frequency-independent Q_p) beneath Kinki region is estimated using t^* determined by applying the S-coda wave spectral ratio method to waveform data from the nationwide dense seismic network and temporary seismic observations beneath Kinki region [Shibutani and Hirahara, 2016]. Method and analysis procedure used in Kita and Matsubara [2016] were adopted in this study. The temporary seismic observation was performed from May 2004 to March 2013. The seismic attenuation structure was imaged beneath Kii peninsula at depths down to 50 km. The resolution of the image was improved comparing to that in the previous study [Kita and Matsubara, 2016 JGR], in which only data from the nationwide dense seismic network was used. Very low- Q_p portion is clearly imaged in the continental plate at depths ~ 30 km beneath from Osaka to southern Kyoto. The location of the very low- Q_p portion corresponds to the location of Low V_p and V_s portion by Shibutani and Hirahara [2016]. Beneath Kii peninsula, hypocenters of low frequency earthquakes determined by Ohta and Ide [2011] are located above relatively low- Q_p portion within the subducting oceanic crust. The location of the relatively low- Q_p beneath the low frequency earthquakes also corresponds to low V_p and low V_s portion obtained by Shibutani and Hirahara [2016]. At the depths of 30 and 50 km, high- Q_p portions are imaged beneath Kumano, Shingu, Kouyasan and Izumi-Ohtsu region. The strike of the high- Q_p region corresponds almost to that of segmentation boundary of V_p/V_s structure [Akuhara et al., 2013] and tremors.

Keywords: Seismic attenuation structure, Slow earthquakes, Seismic velocities structures, t^* , Southwestern Japan

Seismic Attenuation Tomography of Gofar Transform Fault, East Pacific Rise Using OBS Observations

*Haijiang Zhang¹, Jing Hu¹, Hao Guo¹

1. University of Science and Technology of China, School of Earth and Space Sciences

Gofar transform fault of East Pacific Rise generates M_w 5.5-6 large earthquakes quasi-periodically on some segments of the fault, which are separated by stationary rupture barriers. Earthquakes in the seismic cycle of the large earthquake have clear spatial and temporal evolutions. To better understand the relationship between the earthquake behavior and the physical properties of the fault zone along the strike, Woods Hole Oceanographic Institution deployed a broadband ocean bottom seismograph (OBS) array on Gofar transform fault for 1-year continuous measurements, which successfully captured a M_w 6.0 earthquake on 18 September 2008 and provided an unprecedented dataset. By using t^* values determined from fitting seismic waveform frequency spectrum, we have conducted three-dimensional seismic attenuation tomography to determine along-strike attenuation structure. Combined with the high-resolution earthquake locations and V_p , V_s and V_p/V_s models determined from seismic velocity tomography, we found that the seismicity behavior is mainly controlled by structure heterogeneities along the fault.

Keywords: Gofar transform fault, Seismic attenuation tomography, Structure segmentation